Orientation and Dynamics of an Antimicrobial Peptide in the Lipid Bilayer by Solid-State NMR Spectroscopy

Satoru Yamaguchi,* Daniel Huster,* Alan Waring,† Robert I. Lehrer,† William Kearney,‡ Brian F. Tack,‡ and Mei Hong*

*Department of Chemistry, Iowa State University, Ames, Iowa 500112; †Department of Medicine, University of California at Los Angeles School of Medicine, Los Angeles, California 900953; and ‡Department of Microbiology, University of Iowa College of Medicine, Iowa City, Iowa 52242 USA

ABSTRACT The orientation and dynamics of an 18-residue antimicrobial peptide, ovispirin, has been investigated using solid-state NMR spectroscopy. Ovispirin is a cathelicidin-like model peptide (NH_2-KNLRRIIRKIIHIIIKKYG-COOH) with potent, broad-spectrum bactericidal activity. ^{15}N NMR spectra of oriented ovispirin reconstituted into synthetic phospholipids show that the helical peptide is predominantly oriented in the plane of the lipid bilayer, except for a small portion of the helix, possibly at the C-terminus, which deviates from the surface orientation. This suggests differential insertion of the peptide backbone into the lipid bilayer. ^{15}N spectra of both oriented and unoriented peptides show a reduced ^{15}N chemical shift anisotropy at room temperature compared with that of rigid proteins, indicating that the peptide undergoes uniaxial rotational diffusion around the bilayer normal with correlation times shorter than 10^{-4} s. This motion is frozen below the gel-to-liquid crystalline transition temperature of the lipids. Ovispirin interacts strongly with the lipid bilayer, as manifested by the significantly reduced ^2H quadrupolar splittings of perdeuterated palmitoyloleoylphosphatidylcholine acyl chains upon peptide binding. Therefore, ovispirin is a curved helix residing in the membrane-water interface that executes rapid uniaxial rotation. These structural and dynamic features are important for understanding the antimicrobial function of this peptide.

INTRODUCTION

Antimicrobial peptides of mammalian origin are distributed between two broad classes; the cysteine-rich α- and β-defensins and the various cathelicidins. Both classes of peptides have been ascribed pivotal roles in the innate immune responses of mammals (Lehrer et al., 1993; Zasloff, 1987). They are small, positively charged, amphiphilic molecules that are attracted by electrostatic forces to polyanionic structures present in barrier membranes of bacteria. This is viewed as the initiating event on a pathway that ultimately leads to disruption of the membrane (Bessalle et al., 1990; Wade et al., 1990; Yasin et al., 1996). However, the exact mode of interaction of these peptides with the lipid bilayers is still unresolved (Bechinger, 1999; Huang, 2000), and distinct structural models have been proposed. The barrel stave model (Ehrenstein and Lecar, 1977) postulates the formation of transmembrane pores that dissipate the electric potential of the membrane, whereas the carpet model (Oren and Shai, 1998; Pouny et al., 1992) hypothesizes that these peptides rupture the membrane by orienting on the surface of the bilayer and forming an extensive carpet. Other models with intermediate peptide orientations have also been proposed; for example, the toroidal model invokes the formation of torus-like pores by peptide-lipid complexes (Ludtke et al., 1996; Matsuzaki, 1998). To elucidate the molecular mechanisms of the antimicrobial activities of natural and synthetic peptides, it is important to determine the orientation and dynamics of these peptides in lipid bilayers. Such structural information may also facilitate the design of new antimicrobial peptides with desired specificity and potency.

Cathelicidins are primarily found in granules of cells of myeloid lineage. Upon secretion at sites of inflammation by infiltrating neutrophils, cathelicidins are processed by proteolysis giving rise to an N-terminal cathelin domain of unknown function and a C-terminal antimicrobial domain (Gennaro and Zanetti, 2000; Zanetti et al., 1995). Both α-helical and β-sheet motifs have been found among the various antimicrobial domains of cathelicidins (Chen et al., 1995; Roumestand et al., 1998; Schibli et al., 1999). A recent assessment of the bactericidal activities of five mammalian cathelicidin-derived peptides revealed that those of sheep (Smap29) and rabbit (Cap18) manifested potent, broad-spectrum activity irrespective of sodium chloride levels (Travis et al., 2000). $Smap29_{[1–18]}$, an octadecapeptide comprising the first 18 N-terminal residues of Smap29, showed more restricted bactericidal activity that was readily attenuated by moderate to high levels of NaCl. This N-terminal domain of Smap29 was used as a design template for the development of peptides with enhanced bactericidal activities. One peptide, named ovispirin, NH_2-KNLRRIIRKIIHIIIKKYG-COOH, possesses extremely broad-spectrum activity, kills rapidly, and retains activity in the presence of moderate to high salt levels and is thus promising for future therapeutic development (Tack, unpublished data). Ovispirin has a net positive charge of +7 at neutral pH and is highly amphiphilic in its folded form. Its secondary structure in a solution of 40% trifluoroethanol (TFE) has

Received for publication 11 April 2001 and in final form 18 July 2001.

Address reprint requests to Dr. Mei Hong, Department of Chemistry, Gilman 0108, Iowa State University, Ames, IA 50011. Tel.: 515-294-3521; Fax: 515-294-0105; E-mail: mhong@iastate.edu.

0006-3495/01/10/2203/12 $2.00

been determined by high-resolution NMR to be α-helical (Protein Data Bank code 1HU5) (Sawai and Tack, personal communications, 2001), but its mode of binding to lipid bilayers has not been examined.

Solid-state NMR spectroscopy is a powerful tool for determining the structure of membrane-active peptides and proteins, because it allows the study of amorphous and partly mobile biological solids directly in the liquid-crystalline lipid bilayers (Bechinger, 1999; Fu and Cross, 1999; Marassi and Opella, 1998). Orientation-dependent nuclear spin interactions such as ^{15}N chemical shift and ^{15}N-^{1}H dipolar coupling provide exquisite probes of the orientation of membrane peptides relative to the bilayer normal. Correlation of the N-H dipolar coupling and the ^{15}N chemical shift in a two-dimensional (2D) spectrum (Wu et al., 1994) further allows the precise determination of the orientational topology of membrane peptides with multiple ^{15}N labels and even with multiple helical segments (Kim et al., 1998; Marassi et al., 1997). On the other hand, ^{2}H NMR of lipids can yield valuable information on peptide-lipid interactions. Combining a ^{15}N NMR investigation of the peptides with a ^{2}H NMR study of peptide-membrane interactions, we can shed light on the molecular mechanisms for antimicrobial activities. Here we employ ^{15}N, ^{2}H, and ^{31}P NMR to investigate the orientation and dynamics of ovispirin in lipid bilayers.

MATERIALS AND METHODS

Peptide synthesis

Ovispirin (NH_2-KN*L*RR*I*IRKI*IH*IKKY*G*-COOH) with amide ^{15}N labels at L3, I6, I11, I13, and G18 was synthesized using solid-phase peptide chemistry. 0-Fluorenylmethyloxycarbonyl (Fmoc) amino acids and coupling solvents were obtained from PE Biosystems (Foster City, CA) or AnaSpec (San Jose, CA). ^{15}N-labeled amino acids were purchased from Cambridge Isotope Laboratories (Andover, MA) and converted to the Fmoc derivatives (AnaSpec). All organic solvents used for peptide synthesis and purification were high-performance liquid chromatography (HPLC) grade or better. The ^{15}N-labeled peptide was made at a 0.25 mmol scale using FastMoc chemistry (Fields et al., 1991) on an ABI 431A peptide synthesizer. We used pre-derivatized Fmoc-Gly ^{15}N-HMP resin (AnaSpec) and double coupling cycles. The crude product was purified by reverse-phase HPLC on a Vydac C-18 column, using a linear gradient of acetonitrile in dilute (0.1% or 0.85%) trifluoroacetic acid. The molecular weight of the product was confirmed by fast atom bombardment or electrospray mass spectrometry, and its purity was confirmed by capillary electrophoresis and analytical HPLC. Several samples were synthesized for collecting the spectra shown here. Except for one sample, which had a purity of 88–90%, all other samples were over 96% pure.

Membrane sample preparation

Oriented ovispirin membranes were prepared by drying and then hydrating the peptide-lipid mixtures on thin glass plates. 1-Palmitoyl-d_{31}-2-oleoyl-*sn*-glycero-3-phosphocholine (POPC-d_{31}) and 1-palmitoyl-2-oleoyl-*sn*-glycero-3-phosphoglycerol (POPG) (Avanti Polar Lipids, Alabaster, AL) were used for reconstituting the peptide. About 5 mg of purified ovispirin was dissolved in 267 μl of TFE, whereas 35 mg of POPC/POPG mixture (3:1 molar ratio) was co-dissolved in 133 μl of chloroform. The two solutions were combined and deposited onto 25 thin cover glasses of the dimension 16 × 4.5 × 0.15 mm (Electron Microscopy Sciences, Fort Washington, PA). Each cover glass received 16 μl of the solution, yielding a surface concentration of ~0.02 mg/mm^2. Care was taken to avoid spreading the solution off the edge of the plates. The glass plates were allowed to dry in air for 48 h and then rehydrated in a closed chamber containing a saturated solution of sodium sulfate with a relative humidity of 95% for at least 2 days. Subsequently, the plates were stacked and wrapped in Parafilm and stored at 4°C in the same humidity until use. This procedure yielded satisfactory alignment of the membrane, as indicated by the narrow ^{31}P lines of the lipids (see Fig. 2). The hydration level of the oriented peptide-lipid multilayers was determined using polarized Fourier transform infrared-attenuated total reflection spectroscopy (Okamura et al., 1990), by measuring the intensity ratio of the OH stretching band of water to the antisymmetric CH_2 stretching band of the lipids. After 48 h of exposure to the water vapor, the degree of hydration of the lipid-peptide film was found to be 47%, which is sufficient to hydrate the POPC/POPG lipids.

To obtain unoriented ovispirin samples, the peptide and lipid solutions were mixed at the same ratio as above, dried, redissolved in a small amount of deionized water, lyophilized, and finally rehydrated to 30 wt % water relative to the total sample weight. This corresponded to ~20 water molecules per lipid, which is sufficient for hydration (Bechinger and Seelig, 1991; Ulrich and Watts, 1994). The powder sample was transferred as a frozen pellet to a 4-mm magic-angle-spinning (MAS) rotor. The two ends of the rotor were filled with Teflon blocks to reduce the inhomogeneity of the radiofrequency (rf) field.

NMR spectroscopy

The NMR experiments were carried out on a Bruker DSX-400 spectrometer (Karlsruhe, Germany) operating at a resonance frequency of 400.49 MHz for ^{1}H, 40.59 MHz for ^{15}N, 162.13 MHz for ^{31}P, and 61.48 MHz for ^{2}H. A static double-resonance probe and a MAS probe with a 4-mm spinner were used. For the static probe, a 5-mm solenoid rf coil was used for experiments on the unoriented ovispirin sample, and a custom-designed 16 × 4.5 × 4.5-mm rectangular coil was used for oriented samples. The rectangular coil tunes to a frequency range from ^{15}N to ^{31}P on the low-frequency channel, thus allowing both ^{15}N experiments on the peptide and ^{31}P and ^{2}H experiments on the lipids to be carried out.

The ^{15}N chemical shift experiments were optimized by a ^{1}H inverse detection scheme developed recently in our lab (Hong and Yamaguchi, 2001). The experiment involves detecting the ^{1}H magnetization that was transferred from ^{15}N by cross-polarization (CP). To achieve high sensitivity, the ^{1}H signals were detected in the windows of a pulsed spin-lock sequence, yielding a single zero-frequency peak at the center of the spectrum. By maximizing the ^{1}H peak intensity, the ^{1}H-^{15}N CP condition was optimized. We then switched back to ^{15}N detection using the same cable connections. This ^{1}H inverse-detection procedure allowed us to optimize the experimental conditions directly on the membrane samples of interest instead of on model compounds, which often have different probe tuning characteristics. Typical ^{15}N and ^{1}H 90° pulse lengths were 6 μs and 3 μs, respectively. For the 2D dipolar chemical-shift correlation experiment, the MREV-8 sequence (Rhim et al., 1973a,b) was used to decouple the ^{1}H-^{1}H dipolar interaction. The ^{15}N chemical shifts of all spectra were referenced to the isotropic chemical shift of *N*-acetyl-valine, which is 122 ppm relative to liquid NH_3. Indirect referencing through ^{15}N-labeled ubiquitin was used for the static spectra of both oriented and unoriented ovispirin samples. The ^{31}P chemical shifts were referenced to liquid H_3PO_4.

The ^{15}N spectra of oriented samples were typically averaged with 15,000–30,000 scans at recycle delays of 2.5–3 s. The ^{1}H-^{15}N CP contact time was usually 500 μs, except for the CP dependence experiments (see Fig. 4), where the contact time was varied. The typical ^{15}N spectral width

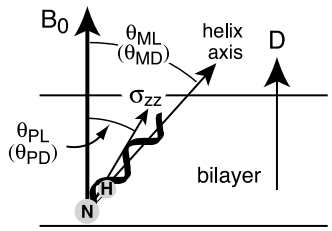

FIGURE 1 Coordinate frames considered in this work. The angle θ_{PL} between the ^{15}N chemical shift main principal axis (σ_{zz}) and the magnetic field (B_0) is directly measured in the ^{15}N experiments. This is approximately equal to the tilt angle of the helix axis from the magnetic field, θ_{ML}. When the lipid bilayers are oriented with the bilayer normal (D) parallel to the magnetic field, then the helix axis tilt from the bilayer normal, θ_{MD}, is identical to θ_{ML}. Similarly, under this condition, $\theta_{PL} = \theta_{PD}$. Randomly oriented bilayers introduce a non-vanishing angle, θ_{DL}, which remove these equalities.

was 40 kHz, and 4–5 ms of time signal was collected. Most experiments were conducted at 293 K unless otherwise specified. The low-temperature ^{15}N experiment was conducted under the same conditions as the room temperature ones, except that the recycle delay was reduced to 1.5 s.

The ^{2}H spectra of POPC-d_{31} were acquired using a quadrupolar echo sequence, with a recycle delay of 0.5 s. A large spectral width of 500 kHz was used for these experiments.

The 2D dipolar chemical-shift correlation spectrum was acquired with 360 scans per t_1 slice, 48 t_1 slices, and a total dipolar evolution time of 1.15 ms. This was sufficient for resolving the scaled N-H dipolar coupling. All spectra were processed with 100–150 Hz line broadening.

Static ^{15}N NMR for helix orientation determination

In this section, we introduce the angular notations used in this paper and briefly summarize the principle of ^{15}N NMR spectroscopy for orientation determination. The extraction of helix orientations in the lipid bilayer is possible due to the orientation dependence of nuclear spin interactions. Specifically, the chemical shift frequency of an amide ^{15}N spin in a peptide depends on the angle (θ_{PL}) between the main principal axis, σ_{zz}, of the chemical shift tensor and the external magnetic field (laboratory frame) (Fig. 1):

$$\omega(\theta_{PL}) = \delta_{iso} + \frac{1}{2}(3\cos^2\theta_{PL} - 1) \times \delta \qquad (1)$$

The ^{15}N chemical shift tensor is roughly axially symmetric. The σ_{zz} axis of the ^{15}N chemical shift tensor is ~17° from the N-H bond, based on model compound studies (Hartzell et al., 1987a,b). The N-H bond is in turn nearly parallel to the helix axis of α-helical peptides (Lehninger et al., 1993). Thus, the σ_{zz} axis of the ^{15}N chemical shift tensor is roughly collinear with the helical axis, and the tilt angle of the ^{15}N chemical shift tensor from the bilayer normal (director frame) (θ_{PD}) or from the magnetic field (θ_{PL}) is approximately equal to the tilt of the helix axis (molecular frame) from the bilayer normal (θ_{MD}) or from the field (θ_{ML}), respectively.

In randomly oriented samples, the ^{15}N signal of each amide exhibits a broad distribution of frequencies due to all possible orientations (θ_{ML}) of the peptide helical axis relative to the magnetic field. Thus, the helix axis orientation relative to the bilayer normal (θ_{MD}) cannot be extracted from the powder spectrum. However, this orientation information can be retrieved if the lipid bilayers are aligned uniaxially, for example, by using glass plates. Due to the uniaxial orientation, the ^{15}N signal resonates at a specific frequency determined by the helix axis orientation relative to the magnetic field. If the bilayer normal of the macroscopically oriented membrane is parallel to the magnetic field, then the tilt of the helix from the magnetic field (θ_{ML}) is identical to the tilt angle from the bilayer normal (θ_{MD}) (Fig. 1). Thus, transmembrane peptides ($\theta_{MD} = 0°$) and surface-oriented peptides ($\theta_{MD} = 90°$) can be readily distinguished.

In addition to the ^{15}N chemical shift interaction, ^{15}N-^{1}H dipolar interaction is another excellent probe of helix orientations in the lipid bilayer. Because the dipolar coupling tensor is exactly along the internuclear vector, the N-H coupling strength reflects the exact orientation of the N-H bond relative to the bilayer normal. Thus, compared with the ^{15}N chemical shift, the N-H dipolar interaction reduces one approximation in the helix orientation determination. The N-H dipolar coupling can be measured by correlating with the ^{15}N chemical shift in a 2D spectrum (Munowitz et al., 1982; Wu et al., 1994).

TABLE 1 ^{15}N chemical shift principal values (±2 ppm) for selectively ^{15}N-labeled ovispirin

^{15}N peak	δ_{iso} (ppm)	σ_{zz} (ppm)	σ_{xx} (ppm)	$\Delta\sigma = \sigma_{zz} - \sigma_{xx}$ (ppm)
Main ovispirin signal*	120	146	74	72
Minor ovispirin signal*	107	104	109	~5
Rigid-limit anisotropy†	119	216	59	157

*These values were measured at 293 K and correspond to motionally averaged tensors.
†These values were measured at 253 K.

Simulations

Simulated 2D N-H dipolar and ^{15}N chemical-shift correlation spectra were calculated for various helix geometries, including the ideal α-helix, the solution NMR coordinates of ovispirin, and the modified coordinates of ovispirin based on the solid-state NMR results here. The helix axis orientation was taken as the average N-H bond orientations. For an ideal α-helix, 18 consecutive residues complete five turns of the helix; thus, the average orientation of the 18 N-H bonds corresponds to the helix axis. Because ovispirin contains only 17 amide groups (not including the N-terminal Lys), the helix axis was approximated as the average orientation of seven consecutive residues, which complete nearly two turns of the helix. After the helix axis was chosen, the N-H bond orientations were expressed in a helix coordinate frame, and the N-H dipolar couplings of individual residues at various tilt angles θ_{MD} were calculated.

In the simulations, a rigid-limit N-H dipolar coupling of 10 kHz corresponding to a bond length of 1.07 Å was used (Roberts et al., 1987). The ^{15}N chemical shift frequency was calculated using an angle of −17° between the σ_{zz} axis and the N-H bond, an angle of 25° between the σ_{xx} axis and the peptide plane (Harbison et al., 1984; Hartzell et al., 1987a,b; Wu et al., 1995), and ^{15}N chemical shift principal values of 64 ppm (σ_{xx}), 77 ppm (σ_{yy}), and 217 (σ_{zz}) ppm (Marassi and Opella, 2000). These correspond to a chemical shift anisotropy (δ) of 98 ppm, an asymmetry parameter (η) of 0.13, and an isotropic chemical shift (δ_{iso}) 119 ppm. For Gly, chemical shift principal values of 41 ppm, 64 ppm, and 211 ppm were used (Lee et al., 1998; Oas et al., 1987). This set of principal values was chosen over other literature values for Gly-containing model compounds (Brender et al., 2001; Lee et al., 1999) because its isotropic shift is close to the measured value of Gly-18 (see Table 1). The calculated DIPSHIFT spectra were searched to find the best fit to the experimental spectrum.

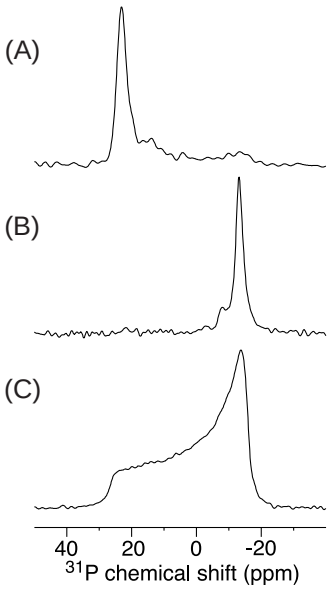

FIGURE 2 ^{31}P spectra of ovispirin-containing POPC/POPG bilayers at a peptide-lipid molar ratio (P/L) of 1:21. (*A*) Oriented sample, with the order axis, which is the lipid bilayer normal, parallel to the magnetic field; (*B*) Oriented sample, with the order axis perpendicular to the field; (*C*) Unoriented sample. The chemical shifts are referenced to an isotropic shift of −0.53 ppm (Pearce and Komoroski, 1993). The spectra were acquired with 32, 32, and 128 scans, respectively.

RESULTS

Qualitative orientation of ovispirin

The determination of ovispirin orientation requires the uniaxial alignment of the lipid membranes containing the peptide. The degree of alignment was assessed by the ^{31}P spectra of the POPC/POPG lipids (Fig. 2). When the peptide-bound membrane was unoriented, the ^{31}P spectrum showed a classical powder distribution (Fig. 2 *C*) characteristic of uniaxially mobile lipids in randomly oriented bilayers.

When the peptide-bound bilayers were oriented and inserted into the magnet with the normal of the glass plates parallel to the field (denoted herein as the 0°-oriented sample), the ^{31}P spectrum exhibits a narrow peak at the downfield edge (24.0 ppm) of the powder spectrum (Fig. 2 *A*). This corresponds to a 0° angle between the motionally averaged ^{31}P chemical shift tensor and the magnetic field. The residual powder intensities are minor in the spectrum, indicating good macroscopic alignment. Based on the peak width, we estimated a mosaic spread of ±4.7° (Nicholson et al., 1987). When the oriented sample was turned so that the alignment axis was perpendicular to the magnetic field (denoted as the 90°-oriented sample in the following), the narrow ^{31}P peak shifted to the upfield edge (−12.4 ppm) of the powder spectrum as expected. The apparently reduced anisotropy (36.4 ppm) between the two limiting orientations compared with the full anisotropy suggests that the phosphate headgroup environment or the lipid dynamics in the oriented sample is somewhat altered by the peptide.

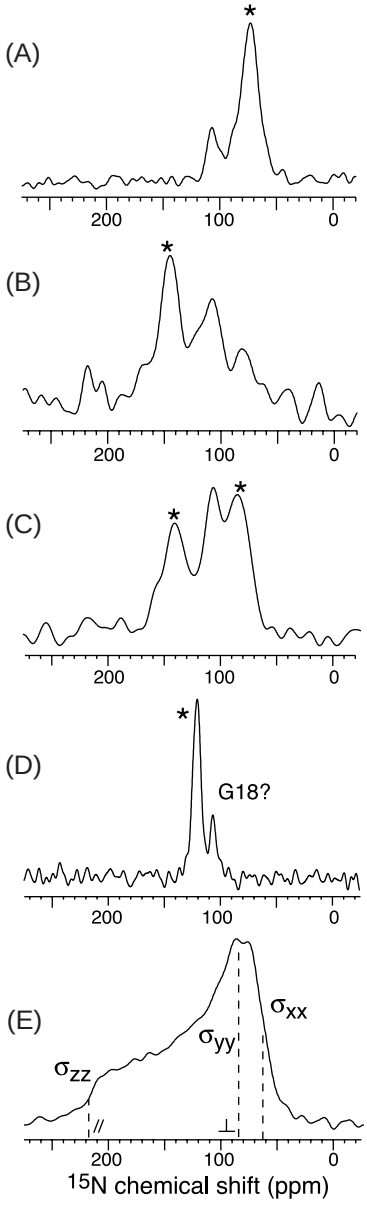

FIGURE 3 ^{15}N spectra of membrane-bound ovispirin at P/L = 1:21. (*A*) Oriented ovispirin, with the order axis parallel to the magnetic field; (*B*) Oriented ovispirin, with the order axis perpendicular to the magnetic field; (*C*) Unoriented ovispirin; (*D*) Unoriented ovispirin under magic-angle spinning. The small peak is tentatively assigned to G18. Spectra *A*–*D* were acquired at 293 K. (*E*) ^{15}N spectrum of unoriented ovispirin at 253 K, below the lipid phase transition temperature. Stars denote the same ^{15}N-labeled residues in the various spectra of ovispirin. ⊥ denotes the in-plane orientation, and // denotes the transmembrane orientation. σ_{xx}, σ_{yy}, and σ_{zz} represent the three principal values of the amide ^{15}N chemical shift tensor. The spectra were acquired with 15,360, 31,744, 26,624, 15,360, and 24,064 scans.

The ^{15}N spectra of ovispirin in the oriented bilayers at a peptide-to-lipid molar ratio (P/L) of 1:21 are shown in Fig. 3, *A* and *B*. For the 0°-oriented sample, the spectrum

showed a dominant signal at 74 ppm and a weaker signal at 109 ppm (Fig. 3 *A*). The main signal corresponds to the upfield edge of the ^{15}N powder spectra of the rigid unoriented ovispirin (see Fig. 3 *E*). For a nearly axially symmetric ^{15}N chemical shift tensor, the lowest frequency results from the 90° orientation between the ^{15}N σ_{zz} axis and the magnetic field, because $\omega(\theta_{PL} = 90°) = \delta_{iso} + (3\cos^2 90° - 1)/2\delta = \delta_{iso} - 0.5\delta$. Thus, most of the labeled ^{15}N-^{1}H bonds are roughly perpendicular to the bilayer normal. In other words, the ovispirin helix mostly resides in the plane of the bilayer. In comparison, the weak ^{15}N signal appears at an intermediate frequency in the ^{15}N chemical shift powder range and will be discussed below.

Ovispirin rotation around the bilayer normal

When the bilayer normal is turned to be perpendicular to the magnetic field, the ^{15}N signals of a surface-residing peptide should shift downfield, because some helical axes are now parallel to the magnetic field, giving the largest possible chemical shift frequency $\omega(\theta_{PL} = 0°) = \delta_{iso} + \delta$. For a typical amide group, this downfield peak should appear at ~217 ppm. Further, because other orientations of the helix are also possible in the bilayer plane, a distribution of ^{15}N chemical shifts is expected. However, the observed ^{15}N spectrum of the 90°-oriented sample (Fig. 3 *b*) showed a relatively narrow frequency distribution, with two peaks at 146 ppm and 106 ppm, much smaller than the predicted value. This can be explained by fast uniaxial rotational diffusion of the peptide around the bilayer normal, which is perpendicular to the molecular axis. If the uniaxial motion occurs on a timescale shorter than ~150 μs, or the inverse of the ^{15}N chemical shift anisotropy, then the orientation dependence of the ^{15}N chemical shift frequency is modified to

$$\omega(\theta_{PD}, \theta_{DL}) = \delta_{iso} + \frac{1}{2}(3\cos^2\theta_{DL} - 1) \times \bar{\delta}$$

$$= \delta_{iso} + \frac{1}{2}(3\cos^2\theta_{DL} - 1) \times \frac{1}{2}\overline{(3\cos^2\theta_{PD} - 1)} \times \delta, \qquad (2)$$

where θ_{DL} is the angle between the bilayer normal and the magnetic field, and the bars denote time averaging. Because θ_{PD} is ~90° for ovispirin, based on the 0°-oriented spectrum (Fig. 3 *A*), the motionally averaged chemical shift anisotropy is $\bar{\delta} \approx 0.5\delta$. Combined with another factor of −0.5 due to $\theta_{DL} = 90°$, we obtain $\omega(\theta_{PD} = \theta_{DL} = 90°) \approx \delta_{iso} + \delta/4$. This corresponds to a ^{15}N chemical shift of 143.5 ppm, in excellent agreement with the observed frequency of 146 ppm for the main signal.

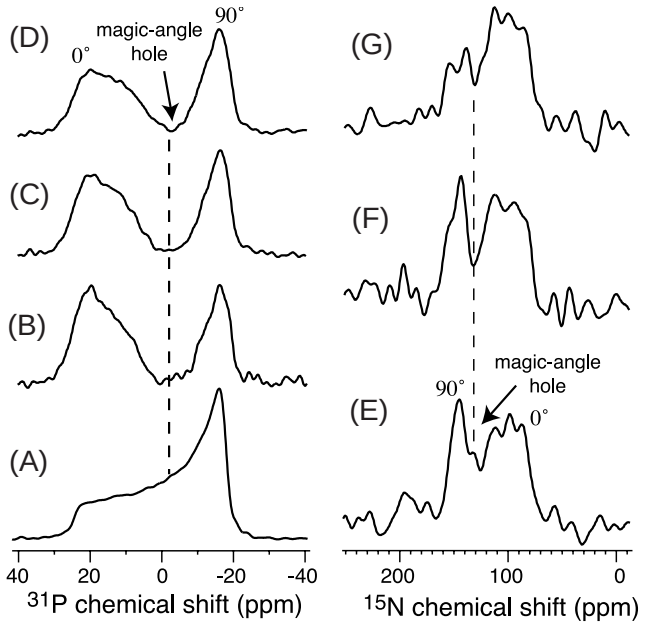

FIGURE 4 Cross-polarization spectra of unoriented POPC/POPG multilayers with bound ovispirin. (*A*) ^{31}P single-pulse spectrum; (*B–D*) ^{31}P CP spectra of the lipids as a function of the ^{1}H-^{31}P CP contact time: 0.5 ms (*B*), 1.0 ms (*C*), and 2.0 ms (*D*). Each CP spectrum was acquired with 128 scans. Note the distinct magic-angle hole and the change in the relative intensities of the 90° and 0° edges of the spectra. (*E–G*) ^{15}N spectra of unoriented ovispirin as a function of the ^{1}H-^{15}N CP contact time: 0.3 ms (*E*), 0.6 ms (*F*), and 1.0 ms (*G*). The numbers of scans were 5120, 5120, and 7168, respectively. Note the reversal of the 90° and 0° edges from the ^{31}P spectra and the resulting different position of the magic-angle hole.

The fast uniaxial rotational diffusion of ovispirin is verified by the ^{15}N spectrum of unoriented ovispirin in the POPC/POPG membrane (Fig. 3 *C*). The ^{15}N powder spectrum ranges from 150 ppm to 75 ppm, which is only about half of the typical span of a rigid-limit ^{15}N chemical shift pattern. This confirms that the motional axis is roughly perpendicular to the helix axis and thus must be the bilayer normal.

The ^{15}N spectrum of the unoriented ovispirin deviates significantly from the $\eta = 0$ lineshape expected for a nearly axially symmetric tensor: it has much reduced intensities at ~123 ppm, and there are three singularities rather than one. This complex lineshape results from the combined effect of the uniaxial rotation of the molecule and the presence of two types of ^{15}N chemical shift tensors among the labeled residues (see below). Uniaxial motion around the bilayer normal averages all spin interaction tensors to be parallel to the bilayer normal. Thus, bilayers that are oriented at the magic angle, 54.7°, to the magnetic field exhibit not only isotropic chemical shifts but also vanishing dipolar couplings. The zero ^{1}H-^{15}N dipolar coupling prohibits ^{1}H-^{15}N cross-polarization, thus giving zero intensities at the isotropic frequency of the ^{15}N CP spectra. For the same reason, the ^{31}P CP spectra of the uniaxially mobile lipids also exhibit a magic-angle hole at their isotropic shifts (Fig. 4, *B–D*). This

contrasts with the directly polarized ^{31}P spectrum (Fig. 4 *A*), which is devoid of a magic-angle hole.

The ^{15}N and ^{31}P CP spectra differ in the position of the magic-angle hole: it appears close to the downfield edge of the ^{15}N spectra (Fig. 4, *E–G*) but close to the upfield edge of the ^{31}P spectra (Fig. 4, *B–D*). This results from the different relative orientations between the rigid-limit tensors and the motional axis (θ_{PD}). Because the helix axis is perpendicular to the bilayer normal, the rigid-limit ^{15}N tensor acquires a negative factor $\overline{(3\cos^2\theta_{PD}-1)}/2$ in Eq. 2. Thus, the 90° edge of the ^{15}N spectra, resulting from those bilayers whose normals are perpendicular to the magnetic field (θ_{DL} = 90°), appears downfield from the isotropic frequency. In contrast, the ^{31}P chemical shift tensor is closer to parallel to the motional axis and contributes a positive scaling factor to the frequency. Therefore, the 90° edge of the ^{31}P spectra is upfield from the isotropic frequency. Because the magic-angle hole at the isotropic frequency lies closer to the 90° edge of the spectra than to the 0° edge, they appear switched between the ^{31}P and the ^{15}N spectra.

The ^{31}P CP spectra of the lipids also help to understand the relative intensity of the 90° and 0° edges of the ^{15}N spectra of the peptide. This relative intensity varies with the CP contact time, due to the competing effects of the orientation-dependent ^{1}H-^{15}N dipolar couplings and the ^{1}H rotating-frame spin lattice relaxation times. The ^{31}P spectra of the lipids (Fig. 4, *B–D*) show a similar contact-time dependence for the 90° and 0° edges as the ^{15}N spectra of the peptide.

The uniaxial rotational diffusion of ovispirin around the bilayer normal at room temperature is frozen when the sample is cooled to below the gel-to-liquid crystalline transition temperature (T_C) of the lipids, which is 271 K for POPC and POPG. At 253 K, the ^{15}N spectrum of the unoriented peptide shows the characteristic lineshape of a rigid, nearly axially symmetric chemical shift tensor, with an anisotropic span of ~160 ppm (Fig. 3 *E*). Thus, the uniaxial motion of ovispirin at room temperature is induced by the liquid crystallinity of the lipids. Interestingly, at 263 K the peptide still exhibits small-amplitude motions, because the ^{15}N chemical shift anisotropy, ~130 ppm (not shown), was slightly smaller than the rigid-limit value. The persistence of peptide motion several degrees below T_C probably results from a reduction or broadening of T_C, which was observed in some membrane peptide mixtures (Gomez-Fernandez et al., 1979; Prenner et al., 1999; Zhang et al., 1995). It may also reflect reduced interactions between the surface-bound peptide and the lipid bilayer, compared with the interactions between a transmembrane peptide and the lipid bilayer (Smith et al., 1994).

Two ^{15}N-^{1}H orientations in ovispirin

In the two ^{15}N spectra of the oriented membrane (Fig. 3, *A* and *B*), a weak signal close to the isotropic shift was observed. This indicates the presence of a minor fraction of N-H bonds that, on average, lie near 55° with respect to the bilayer normal. To examine the origin of these two N-H orientations, we determined the principal values of the two ^{15}N chemical shift tensors. The isotropic chemical shifts were obtained from a MAS spectrum (Fig. 3 *D*), which exhibits two peaks at 120 ppm and 107 ppm. The relative assignment of the two ^{15}N peaks among the oriented, unoriented, and MAS spectra can be made in the following way: if the weak signal (109 ppm) in the spectrum of the 0°-oriented sample (Fig. 3 *A*) has an isotropic shift of 120 ppm (Fig. 3 *D*), then the same residue should resonate at ~125 ppm in the spectrum of the 90°-oriented sample. Because no signal is observed at this frequency (Fig. 3 *B*), the 109-ppm peak in the 0°-oriented spectrum must have an isotropic shift of 107 ppm. This assigns the main signal in the 0°-oriented spectrum (74 ppm), the 90°-oriented spectrum (146 ppm), and the MAS spectrum (120 ppm) to the same residues, which also give rise to the two outer peaks in the static powder spectrum. The remaining weak signal in the two oriented-sample spectra, the MAS spectrum, and the central signal in the powder spectrum, is thus assigned to the remaining residue(s). The chemical shift principal values of the two types of residues in ovispirin are summarized in Table 1. The intensity ratio of the two peaks is ~1:4; thus, one of the five labeled residues has a distinct N-H bond orientation and contributes to the minor peak. Because the characteristic ^{15}N isotropic shifts of Gly are lower than all other amino acids (Wishart et al., 1991), we tentatively assign the weak signal to G18.

The small ^{15}N chemical shift anisotropy of one of the five residues could result from two possibilities. First, part of the peptide may undergo near isotropic motion, yielding a small $\bar{\delta}$. Second, the helix backbone may be distorted so that one of the N-H bonds is accidentally oriented near the magic angle from the bilayer normal. To determine which scenario is true, we measured the ^{1}H-^{1}H dipolar couplings using a ^{1}H T_2-filtered ^{15}N CP experiment. The experiment includes a ^{1}H Hahn echo period, during which ^{1}H-^{1}H dipolar couplings dephase the magnetization, followed by a regular ^{15}N CP sequence. By monitoring the ^{15}N intensities as a function of the Hahn echo delay, the ^{1}H-^{1}H coupling strengths can be estimated. Near isotropic motion should reduce the ^{1}H-^{1}H couplings and lead to a slower decay of the ^{15}N signal. In comparison, an accidental magic-angle orientation of a N-H bond would not affect the H-H dipolar couplings, because the H-H internuclear vectors are most likely not at the magic-angle orientation with respect to the bilayer normal. The strong H-H couplings would then dephase the ^{15}N signals at a similar rate to other ^{15}N-labeled sites. Fig. 5 shows the ^{15}N spectra of the 0°-oriented sample with Hahn echo delays from 1 μs to 15 μs. It can be seen that both peaks decay at similar rates. Fitting the intensities to single-exponential functions (not shown) yielded decay constants of 6.6 ± 2.0 μs for the strong signal and 8.0 ± 1.4 μs for

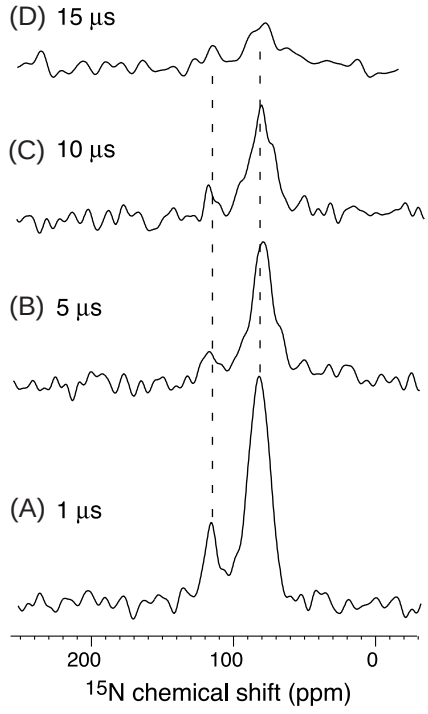

FIGURE 5 ^{15}N CP spectra of 0°-oriented ovispirin as a function of the ^{1}H Hahn echo delays. (*A*) 1 μs; (*B*) 5 μs; (*C*) 10 μs; (*D*) 15 μs. The two peaks decay with similar rates. The spectra were acquired with 5120, 7168, 7168, and 11,264 scans.

the weak signal. Therefore, an isotropic motion of part of the peptide is unlikely to be the cause for the small anisotropy of the minor ^{15}N signal.

We repeated the ^{15}N experiments on two separately synthesized and oriented samples, and the coexistence of two distinct ^{15}N peaks was reproduced. This suggests that heterogeneity of binding or the coexistence of two chemically distinct molecules in the sample is unlikely. Further, the divergent N-H bond orientations cannot be attributed to the formation of unusual lipid phases, because the ^{31}P powder spectrum of the ovispirin-bound membrane (Fig. 2 *C*) exhibits the classical signature of L_α-phase lipid bilayers. Therefore, the most probable reason for the two ^{15}N peaks is a distorted helix with two types of N-H bond orientations relative to the bilayer normal. Based on the tentative assignment of the small peak to G18, we suggest that this distortion occurs toward the C-terminus of the peptide.

Quantitative orientation of ovispirin from 2D dipolar chemical-shift correlation NMR

Because the σ_{zz} axis of the ^{15}N chemical shift tensor actually deviates from the N-H bond by ~17°, a more precise indicator of the N-H bond orientations in the bilayer is the N-H dipolar coupling. Thus, we acquired a 2D N-H dipolar and ^{15}N chemical shift correlation spectrum of ovispirin with the sample alignment axis parallel to the external field (Fig. 6 *A*). Consistent with the 1D ^{15}N spectra, two groups of resonances were observed: the main ^{15}N signals at ~75

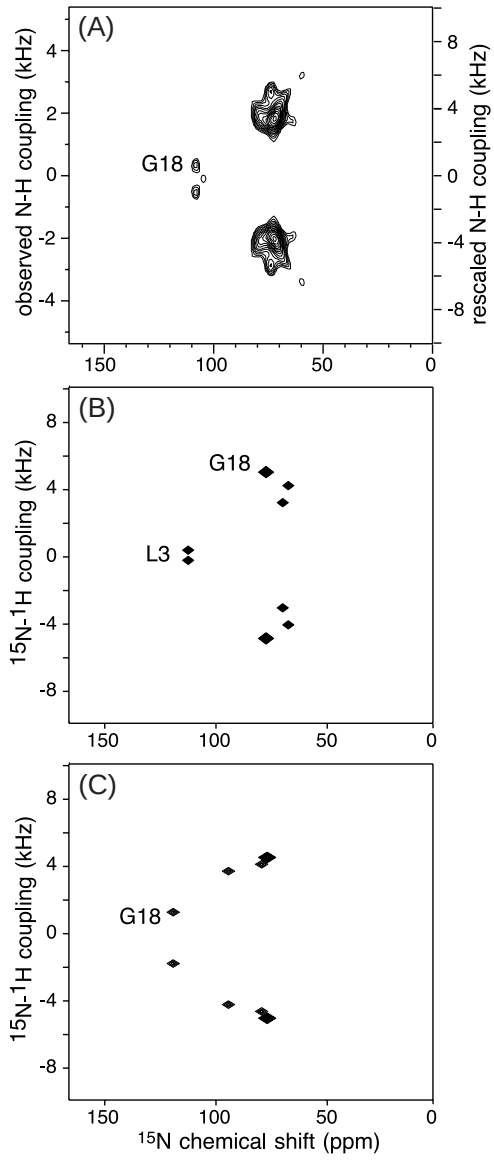

FIGURE 6 (*A*) 2D ^{15}N-^{1}H dipolar and ^{15}N chemical shift correlation spectrum of 0°-oriented ovispirin. The spectrum was acquired with 360 scans per t_1 slice and 48 t_1 slices. The *y* axis shows the MREV-8 scaled dipolar coupling on the left and the full coupling on the right. (*B*) Simulated spectrum using a helix tilt angle of 84° and the solution NMR coordinates of ovispirin (PDB accession code 1HU5). Only the frequencies of the five ^{15}N-labeled residues, L3, I6, I11, I13, and G18, are shown. Note that the downfield ^{15}N peak is assigned to L3 rather than G18, which is the experimental assignment. The larger symbol contains two overlapping peaks. (*C*) Simulated spectrum using the modified ovispirin structure (see text). The large ^{15}N chemical shift now corresponds to G18. The larger symbol contains two overlapping peaks. The simulated spectra in *b* and *c* use the complete N-H couplings for the dipolar dimension and should thus be compared with the right-hand *y* axis in *a*.

ppm show N-H splittings of 3.7–5.4 kHz, whereas the minor ^{15}N peak at 109 ppm has a small splitting of ~0.9 kHz. The exact N-H bond orientations, θ_{NH-D}, can be determined from the dipolar splitting, ω_{NH}, according to

$$\pm\omega_{NH} = 2\delta_{NH} \times \kappa \times \frac{1}{2}(3\cos^2\theta_{NH-D} - 1), \qquad (3)$$

where δ_{NH} is the rigid-limit coupling, and κ is a scaling factor for the homonuclear decoupling sequence. With δ_{NH} = 10 kHz and κ = 0.536 for MREV-8 (Rhim et al., 1973a,b), the large splittings correspond to θ_{NH-D} of 71°–88°, whereas the small splitting corresponds to θ_{NH-D} of ~58°. Thus, the dipolar couplings support the ^{15}N chemical shift spectra for the presence of two distinct types of N-H bond orientations in the peptide. Similarly, the relative intensities of the two regions correspond to a 4:1 ratio between the major orientation and the minor orientation.

Because the N-H bonds are slightly tilted from the helix axis even in ideal α-helices, the N-H bond orientations are not identical to the helix orientation. To extract the latter, one needs to examine the intensity distribution of the 2D spectra of the oriented peptides. It has been shown that, due to the nonlinearity between the ^{15}N chemical shift principal axis and the N-H bond, and between the N-H bond and the helix axis, the peaks of consecutive residues are dispersed in the 2D spectra to form wheel-like patterns whose shape and frequencies reflect the helix tilt (Marassi et al., 2000; Marassi and Opella, 2000; Wang et al., 2000). One consequence of this is that frequency dispersions in the 2D spectra do not necessarily indicate non-ideal helices but could be a result of a finite tilt angle between the helix axis and the bilayer normal. To examine whether this is true for the ovispirin helix, we simulated the dipolar-shift correlation spectra of ideal α-helices for various tilt angles. Our simulations indicate that no ideal α-helices can yield wheel patterns that match the intensity distribution of the oriented ovispirin. The simulated spectra for ideal α-helices require that residues 11 and 18, and residues 6 and 13, fall into two frequency regions separated by ~140° on the helical wheel, whereas residue 3 should have a N-H coupling near the center of the arc. The experimental intensities conflict with these constraints. Therefore, an ideal α-helix geometry is inconsistent with the experimental spectrum, and a distorted helix geometry is required.

To gain more insight into the degree of helix curvature necessary to obtain the 2D spectrum, we calculated the spectrum using the solution structure of ovispirin (Sawai and Tack, personal communications, 2001). Although this solution structure may not be the actual structure of the peptide in the lipid bilayer, it may be treated as a first approximation. We varied the helix tilt angles (τ) from 0° to 90° at 3° increments, and the rotation angles from 0° to 360° at 5° steps. Only solutions with τ between 80° and 90° were found. One of these simulated spectra (Fig. 6 *B*), for τ = 84°, shows reasonable agreement with the experiment spectrum. Because the solution structure of ovispirin is not a straight helix, this strongly suggests that the membrane-bound-state peptide must also be curved to yield the experimental ^{15}N spectra.

However, the simulated 2D spectrum in Fig. 6 *B* assigns the minor peak with the small dipolar splitting to L3. This conflicts with the experimental assignment of the small peak to G18. A helix bent at the C-terminus so that it inserts more deeply into the bilayer would also be more consistent with the hydrophobicity gradient of ovispirin. To test the hypothesis that a C-terminus-bent helix can fit the experimental 2D spectrum, we modified the ovispirin solution structure by changing the ϕ torsion angle of Y17 from −90° to −140°, so that the N-H bond of G18 forms a large angle with the other four labeled N-H bonds. The simulated 2D spectra for the modified structure, for tilt angles between 80° and 90° from the bilayer normal, agree qualitatively with the experimental N-H splittings and ^{15}N chemical shifts. Fig. 6 *C* shows the simulated spectrum for a tilt angle of 90°, where the downfield ^{15}N peak corresponds to G18. The simulation also places the polar and hydrophobic residues at very different depths along the bilayer normal, consistent with the energetically favorable arrangement of placing the hydrophobic residues closer to the bilayer interior and the polar residues closer to the aqueous phase.

Effect of peptide binding on the lipid order

Although the mode of binding to the lipid bilayer is an important aspect in understanding the mechanism of action of ovispirin, the structure and dynamics of lipid bilayers upon peptide binding can also provide useful insights into the antimicrobial functions. ^{2}H NMR is a widely used probe of the conformational disorder of liquid-crystalline lipid bilayers (Koenig et al., 1999; Seelig and Seelig, 1980). We compared the ^{2}H quadrupolar splittings of *sn*-2 chain-perdeuterated POPC in the mixed POPC/POPG membrane in the presence and absence of ovispirin. The ^{2}H spectra of oriented lipids without the peptide (Fig. 7 *A*) exhibits well resolved splittings, which can be converted to an order parameter profile that decreases along the acyl chain with increasing depth (Bloom et al., 1991). The largest quadrupolar splitting ($\Delta\nu_q$) is 62 kHz, which corresponds to an order parameter of ~0.26, and can be assigned to the relatively rigid CD_2 groups closest to the glycerol backbone. The smallest splitting is ~7 kHz and corresponds to the mobile methyl groups at the end of the acyl chains in the core of the bilayer.

Upon the addition of ovispirin, and with the lipid bilayer normal parallel to the magnetic field, we observed a significant reduction of the ^{2}H quadrupolar splittings and a broadening of most peaks (Fig. 7 *B*). Simulation of spectrum (Fig. 7 *B*) yielded reduced order parameters for the entire lipid chain length, ranging from 0.21 to 0.03 (Fig. 7 *C*). This

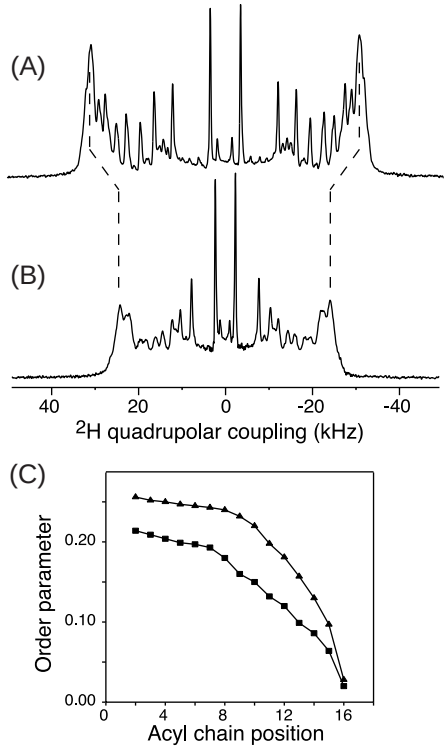

FIGURE 7 ^{2}H spectra of *sn*-2-d_{31}-POPC in oriented POPC/POPG bilayers with the order axis parallel to the field. (*A*) Without ovispirin; (*B*) With ovispirin at P/L = 1:21. A total of 512 scans were co-added for each spectrum. (*C*) ^{2}H order parameter profiles without (▲) and with (■) ovispirin, obtained by simulating the experimental spectra.

increased disorder of the acyl chains in the hydrophobic core of the bilayer is understandable, because binding of ovispirin at the membrane-water interface increases the lipid headgroup area per molecule, allowing more spatial freedom for motion in the acyl chains. Such an increase in the bilayer disorder and fluidity has also been reported recently for other membrane peptides and proteins that possess a predominantly surface component (Huster et al., 2001; Koenig et al., 1999).

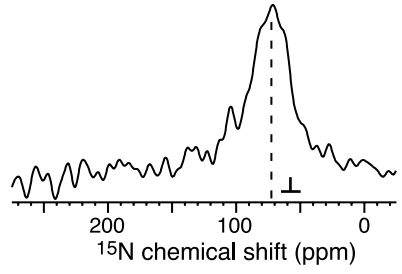

FIGURE 8 ^{15}N spectrum of 0°-oriented ovispirin at P/L = 1:11. The chemical shift of the main peak is 72 ppm; 6144 scans were co-added.

Concentration dependence of ovispirin orientation

The experiments described so far were conducted on membrane samples with P/L = 1:21. To determine whether the ovispirin orientation changes with increasing concentrations of the peptide, we prepared a sample with P/L = 1:11 and recorded its ^{15}N spectra. The spectrum (Fig. 8) showed a peak at 72 ppm, similar to that of the dilute sample, indicating that the in-plane orientation of the peptide persists at this concentration. The resonance was broadened compared with the more dilute sample, with a full width at half-maximum of 30 ppm. This broadening partly resulted from a larger mosaic spread (±12°) of the bilayers, as indicated by the ^{31}P spectrum (not shown). An increased difficulty of orientating the lipid membranes at higher peptide concentrations was also observed for other peptides (Moll and Cross, 1990). In addition, the high concentration of peptide may change the motional characteristics of the sample and reduce the T_2 relaxation time, which can also contribute to the increased linewidths.

DISCUSSION

Disruption of the membrane integrity of foreign cells is considered to be the main mechanism by which antimicrobial peptides achieve their host defense function. This disruption can occur by the formation of peptidic pores, by surface-residing aggregates that fragment the bilayer, or by the formation of non-bilayer peptide-lipid complexes. The ^{15}N solid-state NMR experiments shown here indicate unambiguously that ovispirin is oriented parallel to the plane of the bilayer. More stringently, they show that no segment of the peptide is parallel to the magnetic field when the bilayer normal is aligned with the external field. This rules out not only the barrel-stave model but also the toroidal model for ovispirin function. The latter can be understood by the following argument. In the toroidal model, although the peptide always remains in the plane of the bilayer, its orientation relative to the external magnetic field changes as a function of the local orientation of the bilayer plane. At the inner lining of the torus, the local bilayer surface containing the peptide becomes parallel to the magnetic field; thus, the ^{15}N signal of the peptide should shift downfield. However, no ^{15}N signal was observed at 145 ppm, the maximum downfield frequency expected for this mobile peptide, in the 0°-oriented ^{15}N spectra (Figs. 3 *A* and 8). Similarly, the lipids comprising the inner lining of the torus should exhibit ^{31}P signals distinct from the uniaxial powder pattern (Fig. 2 *C*). The lack of such ^{15}N and ^{31}P signals indicates that there is no detectable amount of peptide-lipid supramolecular pores. Therefore, the carpet model is the most likely mechanism of action for ovispirin. Fig. 9 shows the proposed ovispirin orientation in the lipid bilayer. The peptide is depicted as immersed in the headgroup and glycerol back-

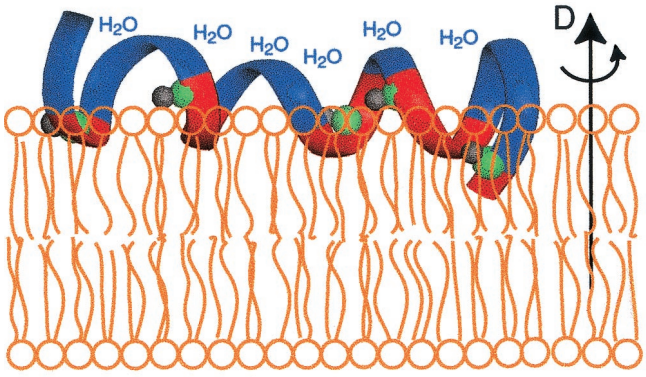

FIGURE 9 Proposed model of ovispirin binding to the lipid bilayer. The structure is based on the TFE-solution structure (PDB code 1HU5) but with a modified Y17 ϕ-torsion angle to produce a C-terminal bend to be consistent with the assignment of the downfield ^{15}N peak to G18. Blue and red represent the hydrophilic and hydrophobic residues, respectively. Green and gray spheres represent the labeled amide ^{15}N sites (L3, I6, I11, I13, and G18) and the corresponding amide protons, respectively. Axis represents the bilayer normal, which is the motional axis for both the peptide and the lipids.

bone region, to satisfy the observed sizeable reduction of the ^{2}H quadrupolar couplings of the POPC acyl chains upon peptide binding.

A number of other membrane peptides with antibiotic activities have also been reported to have surface orientations (Bechinger et al., 1993, 1998; Marassi et al., 1999) and location (Hirsh et al., 1996). The current study adds to this repertoire of in-plane membrane peptides. But ovispirin is unique in the persistence of its orientation even at the very high peptide/lipid molar ratio of 1:11. It has been proposed that antimicrobial peptides undergo a concentration-dependent orientational transition in the lipid bilayer, from a surface orientation to a transmembrane pore (Heller et al., 2000; Huang, 2000). This two-state model has been proposed for magainin and protegrin based on oriented circular dichroism, neutron scattering, and x-ray scattering results (He et al., 1996; Heller et al., 2000; Ludtke et al., 1996). Interestingly, this orientational transition was not observed by solid-state NMR experiments. It is likely that such an orientational transition depends on many environmental factors such as the lipid composition and the peptide/lipid ratio. In the current study, we did not observe such a two-state transition for ovispirin even at very high P/L values. This persistence of the in-plane orientation of ovispirin is consistent with the strong amphipathic nature of this peptide, but it also points to a diversity of structure-function relations among various antimicrobial peptides.

In addition to the orientation of the ovispirin helix with respect to the lipid bilayer, other aspects of the structure and dynamics of ovispirin were observed. First, the ovispirin helix is curved such that one of the five labeled ^{15}N sites has a significantly different N-H bond orientation relative to the bilayer normal. The degree of curvature is comparable to the structure of ovispirin in TFE solution. However, because the simulated 2D spectrum based on the solution structure (Fig. 6 *B*) yielded a different assignment of the small peak from the experimental assignment, the membrane-bound structure of ovispirin most likely differs from the solution structure. We propose an alternative structure, which is curved at the C-terminus (Fig. 9), by modifying the ϕ torsion angle of Y17. This small modification retains all the hydrogen bond distances in the original solution structure except for the CO(I14)–NH(G18) distance, which is increased from 2.71 Å to 3.85 Å. This modified structure reproduces the experimental 2D spectrum qualitatively (Fig. 6 *C*), assigns the downfield ^{15}N chemical shift to G18, maintains the perpendicular orientation of the peptide backbone from the bilayer normal, and places the hydrophobic residues (red in Fig. 9) toward the bilayer and the hydrophilic residues (blue) toward the aqueous phase. Moreover, it is consistent with the hydrophobicity gradient of ovispirin. We hypothesize that ovispirin adopts a structure similar to our model in the membrane-bound state. This raises the intriguing possibility that the antimicrobial function of this peptide may be facilitated by small conformational differences between the solution state and the membrane-bound form.

The membrane-bound ovispirin is not a static molecule. Rather, the entire helix undergoes uniaxial rotational diffusion around the bilayer normal, perpendicular to the helix axis, on a timescale shorter than ~150 μs. This is unambiguously shown by the 90°-oriented ^{15}N spectrum (Fig. 3 *B*), the ^{15}N powder spectrum (Fig. 3 *C*), and the contact-time-dependent CP spectra (Fig. 4, *E–G*). The motion is frozen below the lipid phase transition temperature, as shown by the rigid-limit anisotropy of the ^{15}N spectrum (Fig. 3 *E*). Although uniaxial rotation is known to occur in several other membrane peptides of similar sizes, such as gramicidin (Cornell et al., 1988; Lee et al., 1993), melittin (Smith et al., 1994), and alamethicin (North et al., 1995), most of these peptides exhibit the transmembrane orientation. The closest analogy to ovispirin is the transmembrane domain of the M2 protein from the influenza A virus, which was found to have a significant tilt angle of 32°–38° from the bilayer normal (Song et al., 2000). It also undergoes fast uniaxial rotation around the bilayer normal, as shown by the narrowed ^{15}N lineshape (Fig. 4 *B* in Song et al., 2000) when the bilayer normal was perpendicular to the magnetic field. In the current study, the uniaxial rotation of ovispirin may at first appear surprising, because the peptide lies predominantly in the plane of the bilayer, extending for ~23 Å according to the solution structure. However, when one considers the highly dynamic nature of the liquid-crystalline lipid bilayer, and the fact that ovispirin is only ~2.5 times larger than a lipid molecule, then such a rotational diffusion is quite conceivable. Collisions with the lipid molecules, which undergo constant fast translational and rotational diffusion, can readily induce this motion. Further, the in-plane orientation of the peptide makes it interact with a

large number of lipid molecules and thus more susceptible to the lipid dynamics. Note that this uniaxial rotational diffusion does not contradict the amphipathicity of the peptide, because the motional axis is not the helix axis but rather the bilayer normal. Thus, the hydrophobic face of the peptide remains in contact with the hydrophobic lipid bilayer, and the hydrophilic residues face the water molecules regardless of the motion. To the best of our knowledge, this is the first time that uniaxial rotational diffusion of a surface-bound peptide around the bilayer normal is observed. The persistence of the global motion of ovispirin several degrees below the phase transition temperature of the lipids further underscores the propensity for motion of small membrane peptides. Our understanding of the molecular mechanism of the antimicrobial activity of ovispirin needs to take into account both the orientation and the dynamics of this peptide in the lipid bilayer, as well as the increased disorder of the lipid bilayer.

M.H. thanks the Beckman Foundation for a Young Investigator Award. D.H. is grateful for a postdoctoral fellowship from the BASF AG and the Studienstiftung des deutschen Volkes. R.I.L. is supported by National Institutes of Health grants AI 43934 and AI 22839.

REFERENCES

Bechinger, B. 1999. The structure, dynamics, and orientation of antimicrobial peptides in membranes by multidimensional solid-state NMR spectroscopy. *Biochim. Biophys. Acta.* 1462:157–183.

Bechinger, B., and J. Seelig. 1991. Conformational changes of the phosphatidylcholine headgroup due to membrane dehydration: a ^{2}H-NMR study. *Chem. Phys. Lipids.* 58:1–5.

Bechinger, B., M. Zasloff, and S. J. Opella. 1993. Structure and orientation of the antibiotic peptide magainin in membranes by solid-state nuclear magnetic resonance spectroscopy. *Protein Sci.* 2:2077–2084.

Bechinger, B., M. Zasloff, and S. J. Opella. 1998. Structure and dynamics of the antibiotic peptide PGLa in membranes by solution and solid-state nuclear magnetic resonance spectroscopy. *Biophys. J.* 74:981–987.

Bessalle, R., A. Kapitkovsky, A. Gorea, I. Shalit, and M. Fridkin. 1990. All-D-magainin: chirality, antimicrobial activity and proteolytic resistance. *FEBS Lett.* 274:151–155.

Bloom, M., E. Evans, and O. G. Mouritsen. 1991. Physical properties of the fluid lipid-bilayer component of cell membranes: a perspective. *Q. Rev. Biophys.* 24:293–397.

Brender, J. R., D. M. Taylor, and A. Ramamoorthy. 2001. Orientation of amide-nitrogen-15 chemical shift tensors in peptides: a quantum chemical study. *J. Am. Chem. Soc.* 123:914–922.

Chen, C., R. Brock, F. Luh, P. J. Chou, J. W. Larrick, R. F. Huang, and T. H. Huang. 1995. The solution structure of the active domain of CAP18: a lipopolysaccharide binding protein from rabbit leukocytes. *FEBS Lett.* 370:46–52.

Cornell, B. A., F. Separovic, A. J. Baldassi, and R. Smith. 1988. Conformation and orientation of gramicidin A in oriented lipid bilayers measured by solid-state carbon-^{13}C NMR. *Biophys. J.* 53:67–76.

Ehrenstein, G., and H. Lecar. 1977. Electrically gated channels in lipid bilayers. *Q. Rev. Biophys.* 10:1–34.

Fields, C. G., D. H. Lloyd, R. L. Macdonald, K. M. Ottenson, and R. L. Nobel. 1991. HBTU activation for automated Fmoc solid-phase peptide synthesis. *Peptide Res.* 4:95–101.

Fu, R., and T. A. Cross. 1999. Solid-state nuclear magnetic resonance investigation of protein and polypeptide structure. *Annu. Rev. Biophys. Biomol. Struct.* 28:235–268.

Gennaro, R., and M. Zanetti. 2000. Structural features and biological activities of the cathelicidin-derived antimicrobial peptides. *Biopolymers.* 55:31–49.

Gomez-Fernandez, J. C., F. M. Goni, D. Bach, C. J. Restall, and D. Chapman. 1979. Protein-lipid interactions: a study of (Ca^{2+}-Mg^{2+}) ATPase reconstituted with synthetic phospholipids. *FEBS Lett.* 98: 224–228.

Harbison, G. S., L. W. Jelinski, R. E. Stark, D. A. Torchia, J. Herzfeld, and R. G. Griffin. 1984. ^{15}N chemical shift and ^{15}N-^{13}C dipolar tensors for the peptide bond in [^{1-13}C] glycyl [^{15}N] glycine hydrochloride monohydrate. *J. Magn. Reson.* 60:79–82.

Hartzell, C. J., T. K. Pratum, and G. Drobny. 1987a. Mutual orientation of three magnetic tensors in a polycrystalline dipeptide by dipole-modulated ^{15}N chemical shift spectroscopy. *J. Chem. Phys.* 87: 4324–4331.

Hartzell, C. J., M. Whitfeld, T. G. Oas, and G. P. Drobny. 1987b. Determination of the ^{15}N and ^{13}C chemical shift tensors of L-[^{13}C]alanyl-L-[^{15}N]alanine from the dipole-coupled powder patterns. *J. Am. Chem. Soc.* 109:5966–5969.

He, K., S. J. Ludtke, W. T. Heller, and H. W. Huang. 1996. Mechanism of alamethicin insertion into lipid bilayers. *Biophys. J.* 71:2669–2679.

Heller, W. T., A. J. Waring, R. I. Lehrer, T. A. Harroun, T. M. Weiss, L. Yang, and H. W. Huang. 2000. Membrane-thinning effect of the b-sheet antimicrobial protegrin. *Biochemistry.* 39:139–145.

Hirsh, D. J., J. Hammer, W. L. Maloy, J. Blazyk, and J. Schaefer. 1996. Secondary structure and location of a magainin analogue in synthetic phospholipid bilayers. *Biochemistry.* 35:12733–12741.

Hong, M., and S. Yamaguchi. 2001. Sensitivity-enhanced static ^{15}N NMR of solids by ^{1}H indirect detection. *J. Magn. Reson.* 150:43–48.

Huang, H. W. 2000. Action of antimicrobial peptides: two-state model. *Biochemistry.* 39:8347–8352.

Huster, D., X. Yao, K. Jakes, and M. Hong. 2001. Conformational changes of colicin Ia channel-forming domain upon membrane binding: a solid-state NMR study. *Biophys. J.* In press.

Kim, Y., K. Valentine, S. J. Opella, S. L. Schendel, and W. A. Cramer. 1998. Solid-state NMR studies of the membrane-bound closed state of the colicin E1 channel domain in lipid bilayers. *Protein Sci.* 7:342–348.

Koenig, B. W., J. A. Ferretti, and K. Gawrisch. 1999. Site-specific deuterium order parameters and membrane-bound behavior of a peptide fragment from the intracellular domain of HIV-1 gp41. *Biochemistry.* 38:6327–6334.

Lee, K.-C., W. Hu, and T. A. Cross. 1993. ^{2}H NMR determination of the global correlation time of the gramicidin channel in a lipid bilayer. *Biophys. J.* 65:1162–1167.

Lee, D. K., J. S. Santos, and A. Ramamoorthy. 1999. Application of one-dimensional dipolar shift solid-state NMR spectroscopy to study the backbone conformation of membrane-associated peptides in phospholipid bilayers. *J. Phys. Chem.* 103:8383–8390.

Lee, D. K., R. J. Wittebort, and A. Ramamoorthy. 1998. Characterization of ^{15}N chemical shift and ^{1}H-^{15}N dipolar coupling interactions in a peptide bond of uniaxially oriented and polycrystalline samples by one-dimensional dipolar chemical shift solid-state NMR spectroscopy. *J. Am. Chem. Soc.* 120:8868–8874.

Lehrer, R. I., A. K. Lichtenstein, and T. Ganz. 1993. Defensins: antimicrobial and cytotoxic peptides at mammalian cells. *Annu. Rev. Immunol.* 11:105–128.

Lehninger, A. L., D. L. Nelson, and M. M. Cox. 1993. Principles of Biochemistry. Worth Publishers, New York.

Ludtke, S. J., K. He, W. T. heller, T. A. Harroun, L. Yang, and H. W. Huang. 1996. Membrane pores induced by magainin. *Biochemistry.* 35:13723–13728.

Marassi, F. M., C. Ma, J. J. Gesell, and S. J. Opella. 2000. Three-dimensional solid-state NMR spectroscopy is essential for resolution of resonances from in-plane residues in uniformly ^{15}N-labeled helical membrane proteins in oriented lipid bilayers. *J. Magn. Reson.* 144: 156–161.

Marassi, F., and S. Opella. 1998. NMR structural studies of membrane proteins. *Curr. Opin. Struct. Biol.* 8:640–648.

Marassi, F. M., and S. J. Opella. 2000. A solid-state NMR index of helical membrane protein structure and topology. *J. Magn. Reson.* 144: 150–155.

Marassi, F. M., S. J. Opella, P. Juvvadi, and R. B. Merrifield. 1999. Orientation of cecropin A helices in phospholipid bilayers determined by solid-state NMR spectroscopy. *Biophys. J.* 77:3152–3155.

Marassi, R. M., A. Ramamoorthy, and S. J. Opella. 1997. Complete resolution of the solid state NMR spectrum of a uniformly ^{15}N-labeled membrane protein in phospholipid bilayers. *Proc. Natl. Acad. Sci. U.S.A.* 94:8551–8556.

Matsuzaki, K. 1998. Magainins as paradigm for the mode of action of pore forming polypeptides. *Biochim. Biophys. Acta.* 1376:391–400.

Moll, F., and T. A. Cross. 1990. Optimizing and characterizing alignment of oriented lipid bilayers containing gramicidin D. *Biophys. J.* 57: 351–362.

Munowitz, M., W. P. Aue, and R. G. Griffin. 1982. Two-dimensional separation of dipolar and scaled isotropic chemical shift interactions in magic angle NMR spectra. *J. Chem. Phys.* 77:1686–1689.

Nicholson, L. K., F. Moll, T. E. Mixon, P. V. LoGrasso, J. C. Lay, and T. A. Cross. 1987. Solid-state ^{15}N NMR of oriented lipid bilayer bound gramicidin A. *Biochemistry.* 26:6621–6626.

North, C. L., M. Barranger-Mathys, and D. S. Cafisco. 1995. Membrane orientation of the N-terminal segment of alamethicin determined by solid-state ^{15}N NMR. *Biophys. J.* 69:2392–2397.

Oas, T. G., C. J. Hartzell, F. W. Dahlquist, and G. P. Drobny. 1987. The amide ^{15}N chemical shift tensors of four peptides determined from ^{13}C dipole-coupled chemical shift powder patterns. *J. Am. Chem. Soc.* 109: 5962–5966.

Okamura, E., J. Umemura, and T. Takenaka. 1990. Orientation studies of hydrated dipalmitoylphosphatidylcholine multibilayers by polarized FTIR-ATR spectroscopy. *Biochim. Biophys. Acta.* 1025:94–98.

Oren, Z., and Y. Shai. 1998. Mode of action of linear amphipathic alpha-helical antimicrobial peptides. *Biopolymers.* 47:451–63.

Pearce, J. M., and R. A. Komoroski. 1993. Resolution of phospholipid molecular species by ^{31}P NMR. *Magn. Reson. Med.* 29:724–731.

Pouny, Y., D. Rapaport, A. Mor, P. Nicolas, and Y. Shai. 1992. Interaction of antimicrobial dermaseptin and its fluorescently labeled analogues with phospholipid membranes. *Biochemistry.* 31:12416–12423.

Prenner, E. J., R. N. Lewis, L. H. Kondejewski, R. S. Hodges, and R. N. McElhaney. 1999. Differential scanning calorimetric study of the effect of the antimicrobial peptide gramicidin S on the thermotropic phase behavior of phosphatidylcholine, phosphatidylethanolamine and phosphatidylglycerol lipid bilayer membranes. *Biochim. Biophys. Acta.* 1417: 211–223.

Rhim, W.-K., D. D. Elleman, and R. W. Vaughan. 1973. Analysis of multiple-pulse NMR in solids. *J. Chem. Phys.* 59:3740–3749.

Rhim, W.-K., D. D. Elleman, and R. W. Vaughan. 1973. Enhanced resolution for solid state NMR. *J. Chem. Phys.* 58:1772–1773.

Roberts, J. E., G. S. Harbison, M. G. Munowitz, J. Herzfeld, and R. G. Griffin. 1987. Measurement of heteronuclear bond distances in polycrystalline solids by solid-state NMR techniques. *J. Am. Chem. Soc.* 109:4163–4169.

Roumestand, C., V. Louis, A. Aumelas, G. Grassy, B. Calas, and A. Chavanieu. 1998. Oligomerization of protegrin-1 in the presence of DPC micelles: a proton high-resolution NMR study. *FEBS Lett.* 421:263–267.

Schibli, D. J., P. M. Hwang, and H. J. Vogel. 1999. Structure of the antimicrobial peptide tritrpticin bound to micelles: a distinct membrane-bound peptide fold. *Biochemistry.* 38:16749–16755.

Seelig, J., and A. Seelig. 1980. Lipid conformation in model and biological membranes. *Q. Rev. Biophys.* 13:19–61.

Smith, R., F. Separovic, T. J. Miller, A. Whittaker, F. M. Bennett, B. A. Cornell, and A. Makriyannis. 1994. Structure and orientation of the pore-forming peptide, melittin, in lipid bilayers. *J. Mol. Biol.* 241: 456–466.

Song, Z., F. A. Kovacs, J. Wang, J. K. Denny, S. C. Shekar, J. R. Quine, and T. A. Cross. 2000. Transmembrane domain of M2 protein from influenza A virus studied by solid-state ^{15}N polarization inversion spin exchange at magic angle NMR. *Biophys. J.* 79:767–775.

Travis, S. M., N. N. Anderson, W. R. Forsyth, C. Espiritu, B. D. Conway, E. P. Greenberg, P. B. McCray, R. I. Lehrer, M. J. Welsh, and B. F. Tack. 2000. Bactericidal activity of mammalian cathelicidin-derived peptides. *Infect. Immun.* 68:2748–2755.

Ulrich, A. S., and A. Watts. 1994. Molecular response of the lipid headgroup to bilayer hydration monitored by ^{2}H-NMR. *Biophys. J.* 66: 1441–1449.

Wade, D., A. Boman, B. Wahlin, C. M. Drain, D. Andreu, H. G. Boman, and R. B. Merrifield. 1990. All D-amino acid containing channel forming antibiotic peptides. *Proc. Natl. Acad. Sci. U.S.A.* 87:4761–4765.

Wang, J., J. Denny, C. Tian, S. Kim, Y. Mo, F. Kovacs, Z. Song, K. Nishimura, Z. Gan, R. Fu, J. R. Quine, and T. A. Cross. 2000. Imaging membrane protein helical wheels. *J. Magn. Reson.* 144:162–167.

Wishart, D. S., B. D. Sykes, and F. M. Richards. 1991. Relationship between nuclear magnetic resonance chemical shift and protein secondary structure. *J. Mol. Biol.* 222:311–333.

Wu, C. H., A. Ramamoorthy, L. M. Gierasch, and S. J. Opella. 1995. Simultaneous characterization of the amide ^{1}H chemical shift, ^{1}H-^{15}N dipolar, and ^{15}N chemical shift interaction tensors in a peptide bond by three-dimensional solid-state NMR. *J. Am. Chem. Soc.* 117:6148–6149.

Wu, C. H., A. Ramamoorthy, and S. J. Opella. 1994. High-resolution heteronuclear dipolar solid-state NMR spectroscopy. *J. Magn. Reson. A.* 109:270–272.

Yasin, B., R. I. Lehrer, S. S. L. Harwig, and E. A. Wager. 1996. *Infect. Immun.* 64:4863–4866.

Zanetti, M., R. Gennaro, and D. Romeo. 1995. Cathelicidins: a novel protein family with a common proregion and a variable C-terminal antimicrobial domain. *FEBS Lett.* 374:1–5.

Zasloff, M. 1987. Magainins, a class of antimicrobial peptides from *Xenopus* skin: isolation, characterization of two active forms, and partial cDNA sequence of a precursor. *Proc. Natl. Acad. Sci. U.S.A.* 84: 5449–5453.

Zhang, Y. P., R. N. Lewis, R. S. Hodges, and R. N. McElhaney, 1995. Peptide models of helical hydrophobic transmembrane segments of membrane proteins. II. Differential scanning calorimetric and FTIR spectroscopic studies of the interaction of Ac-K2-(LA)12-K2-amide with phosphatidylcholine bilayers. *Biochemistry.* 34:2362–2371.